Characterization of PET Nanocomposites Produced by Different Melt-Based Production Methods

L. V. Todorov, J. C. Viana

Department of Polymer Engineering, IPC–Institute for Polymers and Composites, University of Minho, 4800-058 Guimarães, Portugal

Received 4 November 2006; accepted 4 April 2007
DOI 10.1002/app.26716
Published online 18 July 2007 in Wiley InterScience (www.interscience.wiley.com).

ABSTRACT: Poly(ethylene terephthalate) (PET) based nanocomposites containing 3 wt % of different nanoparticles (MontMorilloniTe–MMT; titanium dioxide–TiO_2; and silica dioxide–SiO_2) were prepared via two independent procedures: mechanical mixing with subsequent direct injection molding (DIM) and mechanical mixing, followed by extrusion blending and injection molding (EIM). The contributions of nanofillers with respect to pure PET were evaluated. The incorporation of nanofillers reduces the intrinsic viscosity of the polymer matrix when processed by DIM and EIM. SAXS results showed that: MMT layers were intercalated for both processing procedures, but slightly higher for EIM; a better dispersion with smaller agglomerates size is achieved for TiO_2 and SiO_2 nanoparticles for EIM than for DIM. According to the results of DSC analysis, all fillers behave as nucleating agents for PET except SiO_2 that acts as inhibitor in case of DIM procedure. The mechanical behavior was assessed in tensile testing. The mechanical test revealed that the addition of nanoparticles have a slight influence on the elastic modulus and yield stress, but a drastic negative influence on the deformation capabilities of the moldings. The measured optical properties of the moldings gloss and haze are also strongly affected by the presence of nanoparticles. © 2007 Wiley Periodicals, Inc. J Appl Polym Sci 106: 1659–1669, 2007

Key words: poly(ethylene terephthalate); nanocomposites; processing; physical properties

INTRODUCTION

Nowadays one of the most widely used polyester as material for plastic packing (e.g., beverage bottles, cosmetic containers, food, pharmaceutical packaging) is poly(ethylene terephthalate) (PET) because of their good mechanical, barrier and optical properties. PET is considered a high consumption polymer of important commercial interest. PET is a slowly crystallizing polymer that can be obtained with different degrees of crystallinity (0–50%) as a result of specific thermal and/or mechanical treatment to which it is submitted.[1] However, there is some tasting and quality problems of packaged products resulted from daylight exposure.[2,3] Therefore, there is still room for improvement of the optical, barrier, and mechanical properties of PET. One possible and very attractive alternative for this is the replacement of conventional unfilled materials with nanosized particle-filled PET (nanocomposites).

Nanocomposites are a new class of composites that are particle-filled polymers for which at least one dimension of the dispersed particles is in the nanometer range (<100 nm). One can distinguish three types of nanocomposites, depending on how many dimensions of the fillers are in the nanometer range. When the three dimensions are in the order of nanometers, we are dealing with isodimensional nanoparticles, such as fumed spherical silica, titanium dioxide (TiO_2) nanoparticles, and others.[4–7] Particles with two dimensions in the nanometer range form elongated structures, such as in the case of carbon nanotubes or cellulose whiskers.[4,5] The third type of nanoparticles is characterized by only one nanosized dimension, the filler being in the form of platelets of one to a few nanometers thick of hundreds to thousands nanometers long (e.g., nanoclays such as MMT).[8–12] These materials are almost exclusively obtained by the intercalation of the polymer inside the galleries of layered host crystals or preferably by full exfoliation of the layered crystals.

The macroscopic effects of the incorporation of nanoparticles to the polymer matrix are quite remarkable. For example, the mechanical properties, optical, barrier, and fire resistant properties[4] of these new material systems are strongly enhanced depending upon the filler type, its level of concentration, its size, and the polymer production method.[5]

Correspondence to: J. C. Viana (jcv@dep.uminho.pt.).
Contract grant sponsor: DESY.
Contract grant sponsor: DESY and European Commission; contract grant number: DESY-D-II-05-101 EC.
Contract grant sponsor: HASYLAB project.

© 2007 Wiley Periodicals, Inc.
WILEY InterScience® DISCOVER SOMETHING GREAT

Making good samples of polymer matrix nanocomposites is a challenging area that draws considerable efforts in the last years. Researchers have tried a variety of processing techniques to make polymer matrix nanocomposites. These include: exfoliation–adsorption; in situ interactive polymerization; template synthesis; and other approaches.[4,8] All listed production methods are complicated, rather difficult for industrial implementation, and costly. A chosen route is melt blending techniques for direct preparation of polymer nanocomposites, such as extrusion and injection molding, both well known industrial methods with vast practical use. But, if in one side the mixing capability in injection molding is limited, subjecting the polymer at several processing stages (extrusion then injection molding) may induce polymer degradation, which may have a drastic effect on the properties and behavior of the polymer based nanocomposite. However, injection molding as direct processing method for production of polymer nanocomposites allow avoiding previous compounding stages (e.g., extrusion), which brings polymer degradation and additional production expenses.

In this work, the melt processing of PET nanocomposites based on different types of nanoparticles and processing methods is investigated. The selected nanoparticles were: nanoclay (MontMorilloniTe, MMT), fumed silica (SiO_2), and fumed TiO_2. Two production processes are used to mold the different types of PET nanocomposites: direct injection molding (DIM) and extrusion with subsequent injection molding. Processing induced PET degradation is analyzed. The thermal, mechanical, and optical properties of the differently molded PET nanocomposites are also compared.

EXPERIMENTAL

Materials

The PET (reference S41T from Selenis S.A.) has a melt flow index of 63.6 ± 5.2 g × 10 min^{-1}. Different types of nanosized fillers were used:

1. An organic modified nanodispersed layered silicate (MMT) with a primary particle size 100 × 500 × 1 nm and interlayer distance of 2.8 nm (NANOFIL 5, distearyl-dimethyl-ammonium ion exchanged bentonite, from SUD–CHEMIE AG, Germany).
2. A highly dispersed hydrophilic fumed TiO_2 with an average primary particle size of 21 nm (AEROXIDE TiO_2 P25, from Degussa AG, Germany). The nanoparticles consist of approximately 80% anatase and 20% rutile.[13]
3. A hydrophilic fumed silica (SiO_2) with an average primary particle size of 12 nm (AEROSIL 200, from Degussa AG, Germany).

Preparation of PET nanocomposites

The three PET nanocomposites, with contents of 3 wt % of MMT, TiO_2, and SiO_2, respectively, were prepared via two independent preparation procedures:

1. Mechanical mixing with subsequent DIM.
2. Mechanical mixing, followed by extrusion blending and injection molding (EIM).

The nanofillers were independently added to PET dried pellets (with dry air at 170°C for 5 h) and were mechanical blending in a tumbler mixer for 15 min. The PET is very sensitive to thermal, oxidative degradation.[14] In order for avoiding or reduction degradation during extrusion, some authors applied N_2 atmosphere during extrusion, whish is not applicable for IM process. In this work we did not use, because we aimed at objective comparison (at same conditions) of both production procedures.

Extrusion blending

The blends were processed in a counter rotating twin-screw extruder. They were dried in a dry air dehumidifier at 170°C for 5 h before extruding. The temperature profile of the extruder ranged from 220°C (at the feeder) to 245°C (at the die). The screws speed was set at 15 rpm. The extruded material has been cooled from die temperature to room temperature at air ambient. Obtained blends were milled in conventional milling equipment.

Injection molding

The PET nanocomposites were injection molded in an ENGEL T45 machine. Before injection molding, PET blends were dried in a dehumidifier with dry air at 170°C for 5 h. The dried pellets were directly supplied to the injection molding machine hopper (by a vacuum transport system) to avoid contact with room atmosphere. Two different types of moldings were used:

1. Laterally gated rectangular plaques of 64 × 64 × 2 mm for optical studies.
2. Dumbbell-like standard specimens of length of 50 and cross section of 4 × 2 mm for mechanical testing.

All specimens were injection molded with fixed processing conditions listed in Table I.

TABLE I
Injection Moulding Processing Parameters

T_{inj} (°C)	T_w (°C)	P_h (bar)	P_b (bar)	V_{inj} (mm s^{-1})
280	15	35	30	40

T_{inj}, injection temperature; T_w, water temperature; P_h, holding pressure; P_b, back pressure; V_{inj}, injection speed.

These conditions have been chosen after series of preliminary experiments, and found to be as most appropriate to get a good dispersion of nanofillers. Relatively high backpressure (P_b = 30 bar) has been used, increasing shearing actions during the plasticizing phase. A high injection velocity (V_p = 68 mm s^{-1}) was also set up (corresponding to a injection flow rate of 28.3 cm^3 s^{-1}). Other process parameters were set as follow: screw rotation velocity (240 rpm), total plasticizing time (3.4 s), and total cycle time (32 s).

Determination of PET intrinsic viscosity

The intrinsic viscosity measurements were performed to evaluate polymer degradation caused by the several processing steps, according to ASTM D 4603 standard.[15] This method allows the determination of the intrinsic viscosity of a PET sample by measuring the flow time of the solution with a single concentration using the Billmeyer equation [eq. (1)]. An Ubbelohde type viscometer U 4944 2KRK was used. A solvent mixture composed of 60/40 phenol/1,1,2,2-tetrachloroethane was needed to prepare the PET solutions. The PET samples were previously ground to accelerate solubilization. Grounded materials were dried in an oven for 4 h at 170°C to avoid polymer hydrolytic degradation. The humidity presence causes rapidly decrease of equilibrium molar mass M_{ne},[14] which explains the need for careful polymer drying prior preparing of solutions. The polymer composites, prepared with corrected concentration (with 3 wt %) after complete dissolution, were centrifuged for 30 min at 3500 rpm and filtered to remove the formed nanofiller sediment. From the flow time of the pure solvent mixture and the known concentration of polymer solutions, it is possible to obtain the relative (η_{rel}), inherent (η_{inh}), reduced (η_{red}), and intrinsic (η) viscosities as follows:

$$\eta_{rel} = t/t_o \tag{1}$$

$$\eta_{inh0,5\%}^{30°C} = \ln(\eta_{rel})/c$$

$$\eta_{red} = (\eta_{rel} - 1)/c$$

$$\eta = \frac{0.25(\eta_{rel} - 1 + 3\ln(\eta_{rel}))}{c}$$

where t is the flowing time of polymer solution (s), t_o is the flow time of pure solvent mixture (s), and c is the polymer solution concentration (g dL^{-1}).

Characterization techniques

Injection molded and extruded injection molded samples were characterized by small angle X-ray diffraction (SAXS). These experiments were performed under synchrotron X-ray radiation (with a CuKα filter, and a wavelength of λ = 0.15 nm) at HASYLAB, DESY, Hamburg (A2 soft condensed matter beamline). The specimens were positioned perpendicular to the incident X-ray beam with the flow direction pointing upward. For all conditions the distance between the sample and detector was at 1765 mm. Accumulation time was of 20 s. The two-dimensional SAXS patterns were acquired by a MARCCD camera. These patterns were integrated along the equatorial, being plotted Intensity-2Θ curves. Intensities were normalized with respect to the incident X-ray intensity, accumulation time, and specimen thickness. The 2Θ scale was calibrated by means of rattail cornea. The angular and layer spacing values are related through the Bragg's law:

$$\lambda = 2d \sin \Theta \tag{2}$$

where d is spacing between diffraction lattice planes and Θ is the measured diffraction angle. Characterization by SAXS was performed in a 2Θ range of 1 to 4°, corresponding to a lattice spacing range between 8.79 and 2.12 nm.

A Perkin–Elmer DSC-7 running in standard mode was used. The temperature of the cold block was kept at 5°C and the nitrogen purge gas flow rate was 20 cm^3 min^{-1}. Temperature and enthalpic calibrations were carried out according to the DSC7 manual procedures (with indium and lead). The sample weight was around 9 mg for all materials analyzed and 50 mL aluminum pans with holes were used. For evaluating the melting range, heating experiments were performed over all samples, from 30 to 270°C, at a heating rate of 20°C min^{-1}. For these experiments, a base line was obtained with two empty pans, in the same working temperature range and with the same scanning rate.

Both cold crystallization and melting parameters were obtained from the heating scans. The glass transition temperature (T_g) was identified too. Melting (T_m) and cold crystallization (T_{cc}) temperatures were considered to be the maximum of the endothermic and of the exothermic peaks of the thermographs, respectively. The fusion (H_m) and the cold crystallization (H_{cc}) enthalpies were determined from the areas of the melting peaks and crystallization peaks, respectively. The calculation of the relative percentage of crystallinity (χ_c) was based on a two-phase (crystalline–amorphous) peak area method,[1] being given by:

$$\chi_c = \frac{\Delta H_m - \Delta H_{cc}}{\Delta H_f} \tag{3}$$

where ΔH_{cc} is the enthalpy released during cold crystallization, ΔH_m is the enthalpy required for melting, and ΔH_f is the enthalpy of fusion of 100% crystalline PET, taken to be equal[1] to 120 J g^{-1}. The reported results are the average of three samples.

The injection molded dumbbell-like specimens were tested in a universal testing machine Zwick/Roell Z005 in tensile mode. The tests were performed at controlled room temperature of 23°C at a test velocity of 1.5 mm min^{-1} (nominal strain-rate of 0.0013 s^{-1}). At least five specimens of each sample were tested. The mechanical properties envisaged were the elastic modulus (E), yield stress (σ_y), and strain at break (ε_b)

The optical properties measured were the gloss and haze. The gloss was measured at 20, 60, and 85° angles from the normal to the molding surface, according to the ASTM D 523 standard,[16] in a flat surface glossmeter Micro TRI-gloss (Gardner, Germany). Measurements were taken in triplicate for each sample from three moldings of each formulation. All results are expressed as gloss units, relative to a highly polished surface of black glass standard with a value equal to 100. Haze was measured as per ASTM D1003[17] using a Hazemeter XL-211 Hazegard (Gardner), in three samples of molded material systems.

RESULTS AND DISCUSSION

Intrinsic viscosity

The effect of the processing route of the different PET nanocomposites on the intrinsic viscosity, η, are presented in Table II in terms of the percentage of reduction of η of the processed samples with respect to the virgin PET pellets.

The intrinsic viscosity values are related to the average molecular weight by means of the Mark–Houwink equation. In case of extrusion and injection molding of pure PET, the most important polymer degradation mechanism proposed was the oxidation process leading to chain scission.[18] During extrusion, as more complex melt-blending technique, the following processes may occur simultaneously: (1) hydrolysis and condensation (the predominating process depends on the water content); (2) trans-esterification, cycle formation; (3) thermal degradation by ethylene–ester rearrangement; (4) thermal degradation by decomposition of weak points (diethylene glycol); (5) chain scission resulting of oxidation at high oxygen concentration and (6) crosslinking resulting of oxidation at low oxygen concentration. On other hand, oxidation was drastically diminished in the case of injection molding: the polymer was totally confined, but the anaerobic thermal degradation could also occur.[18] As can be observed in Table II, for the selected processing setup, the extrusion of PET resulted in higher reduction of η as compared with DIM (a difference of 2.42%). Similar results have also been already reported.[14,19] The EIM samples are revealing the highest degradation, as would be expectable due to the extended processing history. Additional to degradation caused by processing could be adjoin moisture coming from the specific surface of the milled material being much greater than that of pellets, which could cause some hydrolytic degradation.[20]

TABLE II
Percentage Reduction of the Intrinsic Viscosity of the Processed PET Composite Samples With Respect to the Virgin PET Pellets

Processing	Material	Percentage variations (%)[a]
Extruded	PET	5.18
	PET MMT	14.16
	PET TiO_2	14.40
	PET SiO_2	9.28
Injection moulded (DIM)	PET	2.76
	PET MMT	11.80
	PET TiO_2	5.84
	PET SiO_2	17.68
Extruded injection moulded (EIM)	PET	10.90
	PET MMT	12.09
	PET TiO_2	18.92
	PET SiO_2	21.98

[a] Variation in percentage: $[(\eta_{virgin} - \eta_x)/\eta_{virgin})] \times 100$; where η_x is the intrinsic viscosity of each of the processed PET specimens.

The PET nanocomposites show greater reduction on η for all the studied samples as compared with pure PET for same production procedure. This means that PET nanocomposites are more sensitive to degradation than pure PET. In literature works could be found confirming decreasing of viscosity with increasing concentration of inorganic contents in filled polymers.[9,14] From the results of Table II, the different contribution of three nanofillers type at applied production procedures might be evaluated. Sanches-Solis et al.[9] had suggested that slip between the polymer and filler due to low friction of smooth plates and high shear heating during the melt-compounding process are reasons for elevated degradation. On one hand, MMT is causing higher degradation for extrusion rather than in EIM and DIM procedures. On the other hand, TiO_2 showed the lowest reduction on the intrinsic viscosity for DIM and respectively, similar but significant higher variations for the extrusion and EIM process. Similar trend was obtained for MMT, but seems that TiO_2 is less sensitive to the thermal degradation taking part during injection molding. The decreasing of the intrinsic viscosity of the polymer with increasing TiO_2 concentration after extrusion was already

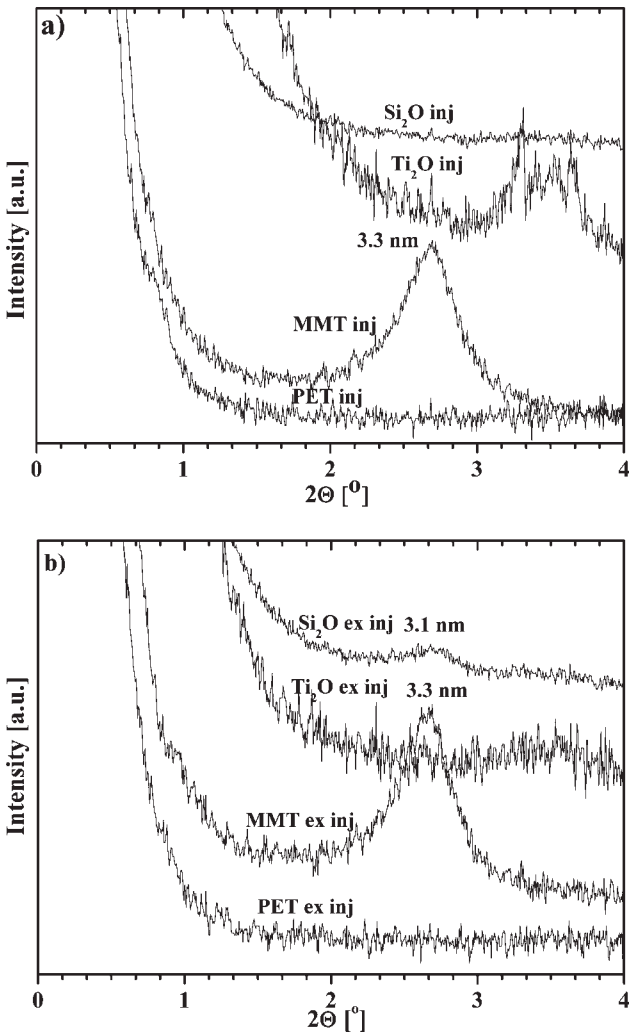

Figure 1 SAXS patterns for PET and PET composites processed by: (a) direct injection molding (inj) and (b) by extrusion–injection molding (ex inj).

reported elsewhere.[21] SiO_2 based nanocomposites are revealing similar behavior as pure PET but showing greater percentage variation values. In case of SiO_2 based PET nanocomposites, the lowest η variation occurs for extrusion and the highest belongs to EIM. For all the cases EIM samples show a higher variation of η, and then higher polymer degradation, as already above-mentioned. PET degradation seems to be a complex process strongly dependent upon the processing history and filler type (e.g., nature, size).

X-ray diffraction studies

Figure 1 shows the SAXS patterns for the PET systems produced by both production procedures. For the directly injected MMT samples, a peak appear at approximately $2\Theta = 2.72^o$ (d = 3.25 nm) [Fig. 1(a)], corresponding to the basal interlayer spacing of the (001) plane of MMT. Pristine MMT shows a basal gallery distance of 2.8 nm ($2\Theta = 3.15^o$). This slight increase in the intergallery spacing indicates that intercalation of MMT occurred, and that the interlayer space of clay increased by 0.45 nm. Therefore obtained nanocomposite is intercalated. Appling of EIM procedure causes slight improved intercalation of MMT, which is confirmed by shift of a peak at $2\Theta = 2.69^o$ (d = 3.28 nm). The relative intensity provides information on the number of scattering structures, regardless of whether they are oriented aggregates or individual sheets. Peak broadness provides information on the scattering domain size distribution (by Scherrer equation). Broader peaks correspond to smaller scattering domains, sharper peaks to larger domains. The SAXS pattern for MMT composite processed by EIM presents a relative intensity decrease and a 4.8% broader intercalation peak with respect to the DIM's one, which indicates higher number of exfoliated clay plates.[21] However, any of used production procedures was sufficient to produce completely exfoliated MMT polymer nanocomposites (lattice spacing higher than 8 nm).[8]

The SAXS patterns of the TiO_2 filled injection molded nanocomposites shows crystalline peaks at $2\Theta = 3.5^\circ$ and $2\Theta = 3.8^\circ$, this peaks in belongs to the anatase structure of titania nano powder and a smaller quantity of rutile, which qualitatively agrees with the crystallographic composition (80% anatase, 20% rutile) of the nanopowder.[13] These peaks are narrower in the case of EIM (Fig. 1) due to the decreased size of scattering domains.

For the SiO_2 filled injection molded samples [Fig. 1(a)], X-ray diffraction pattern did not registered any visible peak in the studied scattering vector range. However, in the case of EMI of SiO_2 based PET composites [Fig. 1(b)] a peak may be observed at approximately $2\Theta = 2.68^\circ$ (3.1 nm). This peak could be attributed to the formation of periodic agglomerates of small SiO_2 crystals that are separated by circa 3.1 nm, as a result of better filler dispersion and orientation inducing during processing.

Differential scanning calorimetry

Figure 2 presents the DSC thermograms of the pure PET and its nanocomposites processed by the different methods.

The values of the glass transition temperature (T_g) cold crystallization peak temperature (T_{cc}), enthalpy of cold crystallization (H_{cc}), melting peak temperature (T_m), enthalpy of melting (H_m), and degree of crystallinity, (χ_c) [calculated from eq. (3)] are listed in Table III.

As observed in Figure 2(a) and also in Table III, the thermograms of extruded material show no presence of cold crystallization peak. This reveals that these specimens are already crystallized as a result

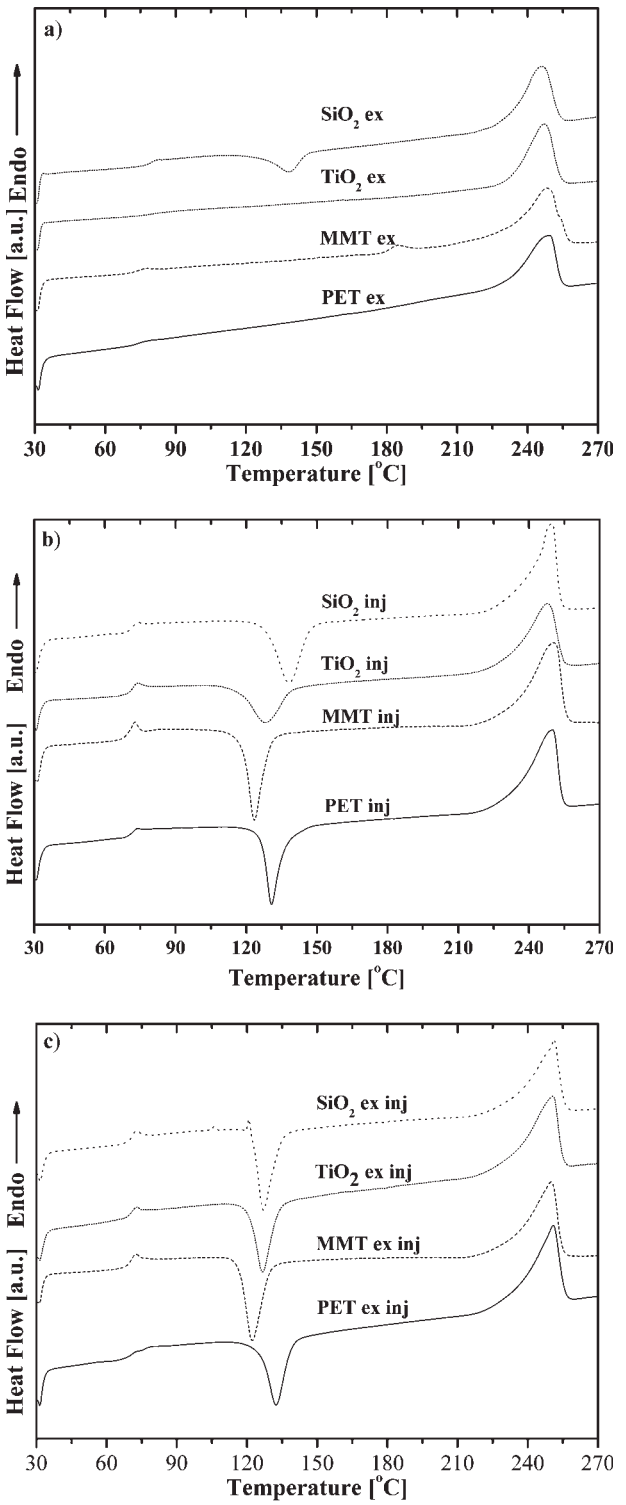

Figure 2 DSC thermograms at 20°C min^{-1} for PET and PET composites processed by: (a) extrusion (ex); (b) injection molding (inj) and (c) by extrusion–injection molding (ex inj).

of the lower cooling rates to which they have been subjected.

A decrement on T_g could be traced in all used production procedures (in average about 1°C) relatively to pure PET. T_g tends also to decrease with the decrement on the size of nanoparticles for amorphous polymers.[5] This tendency is more visible for the extrusion process. Adding of MMT decreases T_g by 1.1°C; use of TiO_2 by 1.6°C and use of SiO_2 by 2.2°C. These variations are less expressive when materials are injected or extrusion–injection molded. On the other hand, MMT composites have lower T_g: 1.9°C and 2.6°C in the case of DIM and EIM with respect to pure polymer for the same production techniques, which could be explained by the presence of intercalated MMT. Difference influence on the T_g may be caused by dissimilar amount of intercalated phase which is lower for DIM. Other works also report that MMT concentration larger than 2 wt % cause a decrease on T_g.[5,10] Moreover, the role of nanofillers should be considered as complex involving shape, nature, particle size effects, and interactions between those.

The presence of nanofillers strongly affects T_{cc}. In DIM the use of MTT decreases T_{cc} by 7.2°C, magnitude also reported by other authors[10]; the use of TiO_2 decreases T_{cc} by 2.5°C. These decrements upon T_{cc} mean that these nanofillers act as nucleating agents for the crystallization process.[19] Single increasing effect on T_{cc} was evidenced by adding SiO_2 nanoparticles with subsequent DIM, with an increment of 7.5°C, corresponding to a crystallization inhibitor activity. On the other side, for the PET SiO_2 composite produced by EIM the filler acts as nucleating agent, decreasing T_{cc}. This may be attributed to the presence of smaller nanoparticle agglomerate size and its better dispersion in polymer matrix achieved during extrusion,[19,22,23] and supported by the SAXS data (Fig. 1). In fact, this nucleating agent effect was observed in all EIM molded PET nanofilled composites leading to a decrease on $T_{cc.}$ For EIM samples, MMT is again the filler with main contribution, decreasing T_{cc} by 10.2°C[10]; TiO_2 reduces T_{cc} by 5.7°C and SiO_2 by 5.3°C. Published results manifest also a close relation between nucleation effect and the filler particles nature and dimensions.[10,19,23]

The different morphological states of the specimens are mainly evidenced in the area of cold crystallization peak, which is characterized by a significant percent of variation (Table III). In a comparison at a fixed processing method, DIM of MMT and SiO_2 filled PET leads to an increment in ΔH_{cc} of 8.7 and 1.8%, respectively. Ou et al.[23] also reported an increment of ΔH_{cc} with increasing organonanoclay concentration in PET nanocomposites. An augmentation of ΔH_{cc} means that the material was initially less crystalline. It appears that adding MMT filler accelerates the crystallization kinetics but the developed crystalline structure is less crystalline, and on the other side SiO_2 acts as a crystallization inhibitor also reducing the degree of crystallinity. Conversely,

TABLE III
DSC Calculated Parameters

Processing	Material	T_g(°C)	T_{cc} (°C)	ΔH_{cc}(J g^{-1})	T_m(°C)	ΔH_m(J g^{-1})	X_c(%)
Extruded	PET	74.6	–	–	249.2	39.2	32.7
	PET MMT	73.5	–	–	248.3	44.8	37.4
	PET TiO_2	73.0	–	–	248.1	39.2	32.7
	PET SiO_2	72.4	–	–	248.8	44.3	37.0
	Var. (%)	3.1	–	–	0.4	14.3	14.3
Injection moulded (DIM)	PET	71.4	130.7	23.6	249.9	42.6	15.8
	PET MMT	69.5	123.5	25.6	250.3	45.8	16.8
	PET TiO_2	71.0	128.2	20.8	247.7	39.4	15.5
	PET SiO_2	71.0	138.2	24.0	249.7	39.9	13.2
	Var. (%)	2.6	11.9	23.2	1.1	16.3	27.2
Extruded injection moulded (EIM)	PET	72.0	132.4	26.1	250.9	42.9	14.0
	PET MMT	69.4	122.2	29.8	249.9	45.4	13.0
	PET TiO_2	70.0	126.7	25.8	250.7	45.5	16.4
	PET SiO_2	70.2	127.1	27.1	251.2	44.2	14.3
	Var. (%)	3.9	8.3	15.6	0.5	6.2	26.7

T_g, glass transition temperature; T_{cc}, cold crystallization peak temperature; H_{cc}, enthalpy of cold crystallization; T_m, melting peak temperature; H_m, enthalpy of melting; X_c, degree of crystallinity (equation 3 with H_f = 120 J g^{-1})[1]; Var, percentage of variation [(max – min)/min)].

the addition of TiO_2 decreases ΔH_{cc} by 11.8%, meaning an initially higher degree of crystallinity of the processed samples. On the other hand, EIM of MMT and SiO_2 increase ΔH_{cc} by 13.4 and 3.9%, respectively. Adding of TiO_2 has almost no influence on ΔH_{cc}.

Negligible variations on the melting peak position were detected in all production methods and nanofillers used. Exception is the incorporation in PET of TiO_2 that leads to a decrease on T_m of 2.2°C in the case of EIM and of 1.1°C for extruded samples. Fray and Boccacini[7] also observed a decrement of T_m with using similar nanofiller; but with a different amount of filler was used.

The absence of the cold crystallization peak corresponds to a higher degree of crystallinity (χ_c) of extruded PET nanocomposite. MMT and SiO_2 fillers increase χ_c[10] by 4.7%, but not affecting the TiO_2 based nanocomposite. Injection molding samples present always a lower χ_c. MMT composites show a slight increasing of χ_c for DIM, but a reduction in the case of EIM. The intercalation of MMT produces an obstacle on the mobility of the macromolecular chains that is, the lamellar space of clay confines the molecular chains movements, which may reduce the ability to crystallize.[24] In fact, our results also point out to decrement of χ_c with a greater amount of intercalated phase (e.g., EIM). DIM production of TiO_2 reflects no changes of χ_c, but EIM causes an increment of 17.4% that could related to the decrease on the filler agglomerate size. The lowest χ_c value (13.2%) for DIM processed samples belongs to SiO_2 nanofiller, that might be related to their crystallization inhibitor character. In the case of EIM, the presence of SiO_2 fillers does not changes χ_c.

Mechanical characterization

Figure 3 presents stress–strain curves for DIM [Fig. 3(a)] and EIM [Fig. 3(b)] specimens of PET and their nanocomposites. Assessed mechanical properties are listed in Table IV. Negligible influenced on the pure PET initial modulus by production procedures is observed. The initial module, E, of MMT-PET composites processed by DIM and EIM also do not vary alike pure PET. In literature, many works reported about a drastic increasing of E with increasing amount of MMT for exfoliated nanocomposites.[8–10] This similar contribution of both production procedures may be due to the lack of exfoliation of nanofiller in the polymer matrix, to a change on the morphological state of the moldings induced by the nanoclay and/or to a high degradation of the PET matrix. Another reason for the improvement of E has been attributed to a strong interaction between matrix and silicate layers via formation of hydrogen bonds.[4] The values in Table IV do not present such strong interaction. In fact, in our case, it is possible that these interactions are reduced due to the organo-modified treatment of the nanoclay (modification by distearyl-dimethyl-ammonium chloride).

The tensile test results for DIM and EIM processed SiO_2 nanocomposites exhibit insignificant diminishing of the stiffness in comparison with pure PET. Some authors refer slightly higher modulus by preparing various silica polymer nanocomposites and little difference between composites with different particle sizes and production methods.[5] This was not confirmed in the present work might because of the different production procedures, particles sizes and polymer nature. TiO_2 injection molded nanocompo-

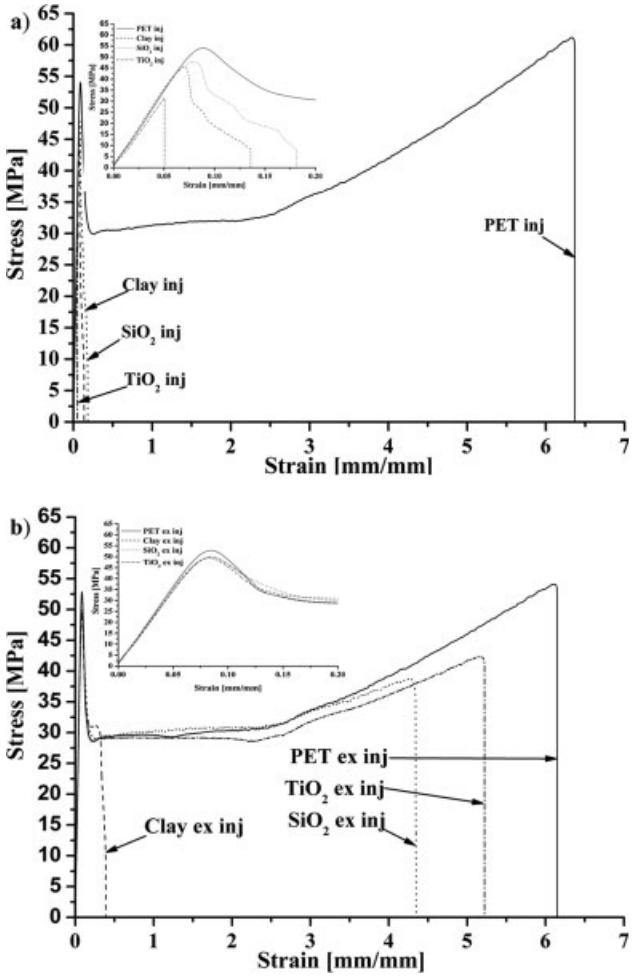

Figure 3 Experimental stress–strain curves for pure PET and its nanocomposites processed by: (a) direct injection molding (inj); and (b) extrusion followed by injection molding (ex inj).

site exhibit the lowest modulus from all compared nanocomposites. The decreasing of agglomerates size by applying EIM improves the initial modulus of TiO_2-PET in comparison with DIM procedure. Straightforward relation between initial modulus and nature, shape and particle size was not distinguished in attained results. The filler concentration could be suggested as most important parameter controlling the material stiffness, and not the production technique, neither the filler nature.

The yield stress of pure PET shows also no dependences upon the used processing techniques. In respect to pure polymer, MMT composites molded by DIM show a reduction of σ_y of −16.2% and EIM of −10.7%. The addition of SiO_2 particles also decreases the yield stress by comparison with pure polymer matrix for the same production technique, respectively, −10.8% for DIM and −8.5% for EIM. Injection molded TiO_2 composite do not show a yield point, showing a highly brittle behavior. EIM of TiO_2 composite reduces by 8.8% the yield stress compared with pure PET. All type of nanofillers used in this study induce a decrease of the yield stress with respect to pure PET. The bad dispersion of the nanofillers, the presence of agglomerated particles that act as stress concentrators and the lack of interaction between particles and polymer matrix may contribute to this.[5] The higher values of σ_y of MMT-PET composite molded by EIM procedure could be attributed to an higher amount of exfoliated MMT as compared with the DIM. Furthermore, in some studies the yield stress was found to increase slightly with decreasing size of the nanoparticles.[5]

The results shown in Table IV for pure PET reveal a strong influence of the production procedures on the strain at break values. Injection molded PET has 61.1% higher ε_b than the EIM of PET that may be due to the significant degradation caused by this production procedure, as already abovementioned. The influence of nanofillers on the deformation capabilities of the moldings is clearly evidenced by the distinct strain at break shown by the moldings. The strain at break diminishes drastically with respect to that of PET in both molded MMT nanocomposites (Fig. 3). Sanches-Solis et al. has shown that strain at

TABLE IV
Mechanical Test Values

Processing	Material	E (MPa)	σ_y (MPa)	ε_b (%)
Direct injection moulded (DIM)	PET	889.2 ± 19.3	55.2 ± 0.8	524.1 ± 15.8
	PET MMT	871.4 ± 12.8	47.1 ± 1.3	11.2 ± 0.7
	PET TiO_2	803.1 ± 9.9	37.2 ± 2.4[a]	5.2 ± 0.3
	PET SiO_2	861.3 ± 21.3	49.5 ± 0.2	16.7 ± 2.4
	Var. (%)	10.7	17.3	10056.6
Extruded injection moulded (EIM)	PET	892.4 ± 6.8	55.8 ± 1.1	475.2 ± 56.5
	PET MMT	865.5 ± 20.1	49.8 ± 0.9	31.0 ± 4.6
	PET TiO_2	866.1 ± 5.4	51.0 ± 1.1	421.9 ± 35.9
	PET SiO_2	866.2 ± 16.6	50.9 ± 1.2	355.9 ± 10.7
	Var. (%)	3.1	12.1	1434.4

E, Initial modulus; σ_y, Yeild stress; ε_b, Strain at break; Var, Percentage of variation [(max – min)/min].
[a] Fracture stress.

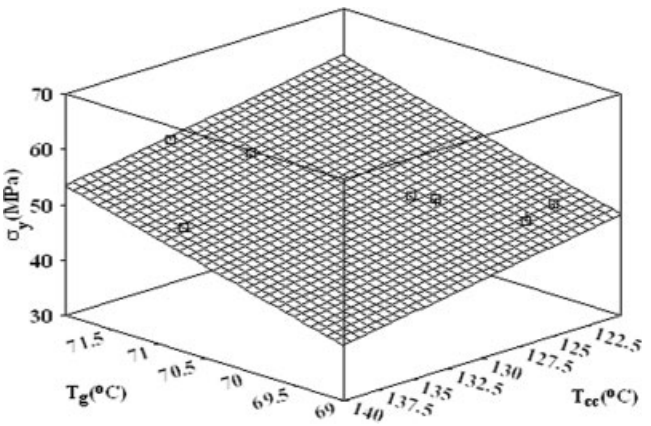

Figure 4 Variation of yield stress, σ_y, glass transition temperature, T_g, and cold crystallization temperature, T_{cc}. (the plane is a linear fit to the data: $\sigma_y = -210.05 + 4.46T_{cc} - 0.41T_g$; $R^2 = 0.89$).

break diminishes drastically for clay composites with their contents of 1, 2, and 3% for organo-modified and nonmodified MMT.[9] The improvement with 24.9% of ε_b for MMT—EIM in comparison with DIM molded composite may be related to the higher amount of exfoliated inorganic nanoparticles. The SiO_2 and TiO_2 nanocomposites produced by DIM show a marked decreasing of deformation capability with respect to PET molded with identical thermomechanical conditions. EIM nanocomposites present also a decrease on ε_b. Fray and Boccacini[7] have reported an improvement on the strain at break with 300% for 0.13 vol % of TiO_2 nanofiller content in PET matrix. The strain at break seems to be very sensitive to the dispersion satte and size of the nanoparticles agglomerates, as would be expected.

The possible reasons for different influence of the production procedure on mechanical properties could be explained by the lack of dispersion and agglomeration formation in case of DIM, and better dispersion for two step procedure (EIM) as a result of applied higher shearing levels. Besides, this will be also accompanied expectantly by strong matrix degradation that may significantly reduce their mechanical properties.

Relationship between yield stress, σ_y, and the glass transition temperature, T_g, and the temperature of cold crystallization, T_{cc} was established (Fig. 4). The σ_y value for DIM TiO_2-PET composite was excluded because of not presence of yielding phenomena in this case. The yield stress increases with T_g and the decrement of T_{cc}. This reflects, for this particular case, a strong dependence of σ_y on the amount and molecular orientation of amorphous phase. This reveals the importance of the amorphous phase for the yielding phenomena. Furthermore, the relative high coefficient of multiple correlation, R^2, means that other morphological parameters are insignificant for the yield stress.

Optical properties

Gloss characterization

The gloss of the molded samples was measured at 20° and 60° and 85° as a function of processing technique and type of nanofiller. According to ASTM standard,[16] the values further considered values will be the measured at 20° because of the high gloss (greater than 70 gloss units) of the samples exposed at 60°. The measured glosses are depicted in Figure 5, for both processing procedures and filler type. The glosses of the samples are related with the surface topology developed during the processing. From Figure 5 could be judged that all nanofillers cause a reduction in gloss with respect to pure PET for both processing procedures. EIM pure PET reduces significantly the specimen gloss as compared with DIM and their relatively higher level of degradation becomes apparent in samples yellowishing. For both processing procedures, the lowest gloss is achieved by the use of SiO_2 nanoparticles, which for DIM decrease gloss of pure PET 59.2% and for EIM by

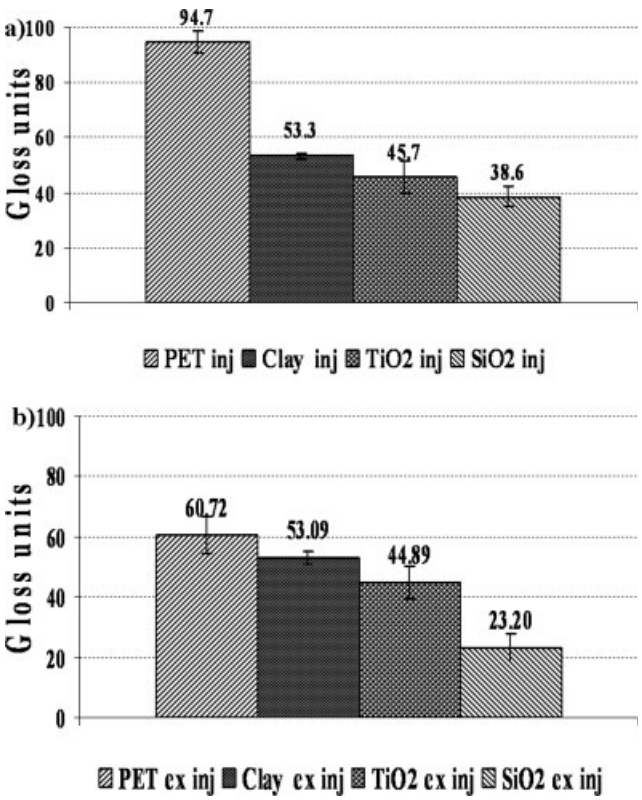

Figure 5 Gloss measurements of pure PET and its nanocomposites processed by: (a) injection molding (inj); and (b) extrusion injection molding (ex inj).

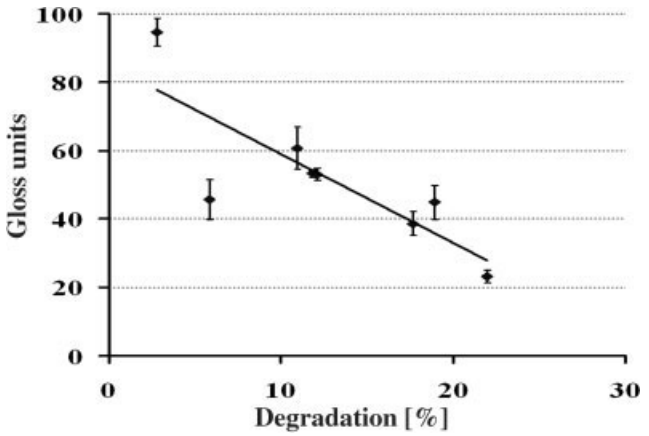

Figure 6 Dependence of gloss and degradation ratio (solid line is a linear fit to the data: Gloss = −2.59 Degradation; $R^2 = 0.67$).

61.8%. The gloss is almost independent of processing technique for MMT and TiO_2 PET composites.

In this sense, the polymer properties (e.g., viscosity), the type of nanofiller and the processing technique all play an important role in the surface roughness, thus determining the specular reflectance characteristics of the air–sample interface: the higher the surface roughness, the lower the gloss.[25] Figure 6 shows the variation of the gloss with the degradation ratio as measured by the variations on the intrinsic viscosity, both being related by a straight line. An increment of polymer degradation results in a decrease on the glossiness, as shown in Figure 6.

Haze

Haze describe the transparency of a material and can be defined as the percentage of the total transmitted light that, in passing through the specimen, is scattered from the incident beam by an angle greater than[25] 2.5°. In practice, a reduction in the contrast of an object viewed through a specimen could be due to an increase of haze. Detected haze for pure PET directly injection molded was of (8.7 ± 1.0)%, this being the unique condition having a haze value lower than 30% (limit value associated with a transparent polymer). The rest of conditions, both DIM and EIM, have a haze value greater than 30%, which respond to diffusing or translucent samples (following the ASTM standard[17]). According to proposed microstructure models used for calculation of transparency[25] the elevated haze of EIM pure PET material is the result of appearance of degraded particles in bulk polymer, which are originating more scattering. Nanofillers in general are increasing slightly haziness, that is directly related to filler size and sample thickness.[19]

CONCLUSIONS

The structure of the polymer was varied by two production procedures (direct injection molding, DIM, and extrusion blending followed by injection molding, EIM) and different types of nanofillers. The PET nanocomposites are more sensitive to degradation than virgin PET, caused by presence of the nanofillers, which are inducing chain scission process leading to a reduction on the average molecular weight and respectively, on the intrinsic viscosity. All the EIM samples show a higher variation of η, and then higher polymer degradation during processing.

Both production procedures are suitable for production intercalated MMT, but slightly higher amount of intercalated phase for EIM is detected. Better dispersion in the polymer matrix of TiO_2 and SiO_2 nanoparticles was also obtained for EIM as compared with DIM, as would be expected. The different processing procedures represented slight influence on T_g and negligible upon T_m. In case of DIM, MMT, and TiO_2 are acting as nucleating agents, but SiO_2 particles behave as crystallization inhibitor. This nucleating effect was exposed by all used inorganic fillers for EIM procedure, that is originated by the better nanofillers dispersion. σ_y increases with T_g and respectively, decrease with the raise of the cold crystallization peak position. The strain at break is related mainly with dispersion: better dispersion result in improved ε_b. Gloss is affected mainly by filler presence and small processing influence is reported. All nanofillers strongly increasing sample haziness.

The authors thank Selenis S.A.–Portugal for providing PET used in this research and Degussa AG–Germany for the AEROSIL 200 and AEROXIDE TiO_2 P25. Funding through FEDER and POCTI programs is acknowledged.

References

1. Viana, J. C.; Alves, N. M.; Mano, J. F. Polym Eng Sci 2004, 44, 2174.
2. Moyssiadi, T.; Badeka, A.; Kondyli, E.; Vakirtzi, T.; Savvaidis, I.; Kontominas, M. G. Int Dairy J 2004, 13, 429.
3. Jenkins, W. A.; Harrington, J. P. Packing Foods with Plastics; Technomic Publishing: Lancaster, PA, 1991.
4. Ray, S. S.; Okamoto, M. Prog Polym Sci 2003, 28, 1539.
5. Jordan, J.; Jacob, K. I.; Tannenbaum, R.; Sharaf, M. A.; Jasiuk, I. Mater Sci Eng A 2005, 393, 1.
6. Petrovic, Z. S.; Cho, Y. J.; Javni, I.; Magonov, S.; Yerina, N.; Schaefer, D. W.; Ilavsky, J.; Waddon, A. Polymer 2004, 45, 4285.
7. Fray, M. E.; Boccacini, A. R. Mater Lett 2005, 59, 2300.
8. Alexandre, M.; Dubois, P. Polym Eng Sci 2000, 28, 1.
9. Sanchez-Solis, A.; Romero-Ibarra, I.; Estrada, R. M.; Calderas, F.; Monero, O. Polym Eng Sci 2004, 44, 1094.
10. Sanchez-Solis, A.; Garcia-Rejon, A.; Manero, O. Macromol Symp 2003, 192, 281.

11. Ou, C. F.; Ho, M. T.; Lin, J. R. J Appl Polym Sci 2004, 91, 130.
12. Nam, P. H.; Maiti, P.; Okamoto, M.; Kotana, T.; Hasegawa, N.; Usuki, A. Polymer 2001, 42, 9633.
13. Boccaccinia, A. R.; Gerhardta, L. C.; Rebelinga, S.; Blakera, J. J. Compos A 2005, 36, 721.
14. Assadi, R.; Colin, X.; Verdu, J. Polymer 2004, 45, 4403.
15. ASTM standard D4603-96. Standard test method for determining inherent viscosity of Poly(ethylene terephthalate) (PET) by glass capillary viscosimeter; Annual Book of ASTM Standards, West Conshohocken, PA, 2000; p 104.
16. ASTM standard D523–85. Standard test method for specular gloss; Annual Book of ASTM Standards, West Conshohocken, PA, 1985; p 121.
17. ASTM Standard D1003–63. Standard test method for haze and luminous transmittance of transparent plastics; Annual Book of ASTM Standards, West Conshohocken, PA, 1961; p 365.
18. Colin, X.; Verdu, J. C R Chim 2006, 9, 1380.
19. Taniguchi, A.; Cakmak, M. Polymer 2004, 45, 6647.
20. Torres, N.; Robin, J. J.; Boutevin, B. Eur Polym J 2000, 36, 2075.
21. Tollea, T. B.; Andersonb, D. P. Compos Sci Technol 2002, 62, 1033.
22. Esteves, A. C. C.; Barros-Timmons, A. M.; Martins, J. A.; Zhang, J.; Cruz-Pinto, W.; Trindade, T. Compos B 2005, 36, 51.
23. Ou, C. F.; Ho, M. T.; Lin, J. R. J Appl Polym Sci 2004, 91, 130.
24. Ou, C. F.; Ho, M. T.; Lin, J. R. J Polym Res 2003, 10, 127.
25. Meeten, G. H. Optical Properties of Polymers; Elsevier Applied Science: London, 1986.